Geosmin–producing *Scytonema foetidum* sp. nov. (Scytonemataceae, Cyanobacteria): morphology and molecular phylogeny

Wittaya Tawong[1,2*], Pongsanat Pongcharoen[1,2] & Tomohiro Nishimura[3]

[1] *Department of Agricultural Science, Faculty of Agricultural Natural Resources and Environment, Naresuan University, Phitsanulok 65000, Thailand; *Corresponding author e–mail: wittayat@nu.ac.th*

[2] *Center of Excellence in Research in Agricultural Biotechnology, Naresuan University, Phitsanulok 65000, Thailand*

[3] *Cawthron Institute, Nelson 7010, New Zealand*

Abstract: A novel *Scytonema* species, *Scytonema foetidum* sp. nov. is described by combining morphological and genetic evidences. Two clonal strains of the new species were isolated from a wet soil sample taken from the Khek River in the lower northern part of Thailand. This species is morphologically similar to *S. hofmanii*, but can be differentiated by a small filament width, conically rounded apical cell, and sheath present throughout the whole trichome. The 16S ribosomal RNA (rRNA), rbcLX, and nifH phylogenetic trees indicated that *S. foetidum* clearly formed a unique cluster within the *Scytonema* sensu stricto clade and shared low 16S rRNA sequence similarity (<98.4%) with the phylogenetically related taxa, supporting separation at species level. The 16S–23S rRNA internal transcribed spacer (ITS) sequences of *S. foetidum* also possessed unique secondary structures in D1–D1′, Box B, and V3 helices, differentiating this species from other known *Scytonema* species. Furthermore, *S. foetidum* could produce the odoriferous compound, geosmin.

Key words: Cyanobacteria, Geosmin, 16S rRNA phylogeny, ITS secondary structure, *Scytonema*, Systematics, Taxonomy, Thailand

Introduction

Cyanobacteria are a group of photosynthetic bacteria comprising numerous genera and species that are found in diverse aquatic (oceans and freshwater) or terrestrial (bare rock and soil) environments (Whitton 2012). An increasing number of cyanobacteria species are now known to produce potent secondary metabolite compounds (i.e. toxins or odoriferous compounds) that can impact terrestrial and water–based organisms, as well as the drinking–water supply (Wu et al. 2012; Catherine et al. 2013; Wang et al. 2019). Most cyanobacteria known as odoriferous compound producers, are filamentous taxa belonging to the orders Nostocales and Oscillatoriales (Suurnäkki et al. 2015; Kim et al. 2018; Tawong et al. 2017, 2019; Wang et al. 2019; Churro et al. 2020), although some species in the order Synechococcales such as *Coelosphaerium* sp. have been reported as the cause of the musty odor in Lake Shinji, Japan (Godo et al. 2017; Hayashi et al. 2019).

Morphological proficiency is important and necessary for cyanobacterial identification, and heterocytous cyanobacteria have been proven to include many morphologically well–defined species or genera. Nonetheless, it is evident that morphological characteristics traditionally used to separate genera and species are not properly related to molecular phylogenetic patterns. To delimitate cyanobacterial species or genus, especially with regards to cryptic taxa, modern cyanobacteria taxonomy has been proposed based on a polyphasic approach (Johansen & Casamatta 2005; Komárek et al. 2014) combining morphological, ecophysiological, biochemical and molecular characteristics (Rajaniemi et al. 2005; Willame et al. 2006). With the development of DNA sequencing, the 16S ribosomal RNA (rRNA) has been widely used as a molecular marker to provide genetic characterization of new cyanobacterial taxa, while the secondary folding structure of the internal transcribed spacer (ITS) also provides molecular evidence to separate taxa at the species level. The ribulose–1,5–bisphosphate carboxylase/oxygenase large subunit gene and the chaperonin–like protein gene (rbcLX) as well as the gene associated with nitrogen fixation (nif gene) are preferred as genetic evidence when discriminating closely related cyanobacteria species and in phylogenetic studies because the evidence for lateral gene transfer is missing only in conserved (core) genes (Palinska &

Surosz 2014; Tawong et al. 2017; Choi et al. 2018). Furthermore, analyses of genes related to biochemical (i.e. cyanobactoxin and pigment) and ecophysiological characteristcs should also be considered for exact classification (Rajaniemi et al. 2005; Tanabe et al. 2007; Sendall & McGregor 2018; Żyszka–Haberecht et al. 2019).

Within the cyanobacterial group, the order Nostocales is a huge monophyletic cluster of filamentous cyanobacteria involving unbranched, false– and true–branched type (Komárek et al. 2014). The family Scytonemataceae is a classical false–branching cyanobacterial group of Nostocales consisting of several genera including *Scytonema*, *Brasilonema*, *Ewamiania*, *Iningainema*, *Scytonematopsis*, *Chakia*, *Ophiothrix*, and *Petalonema* (Bornet & Flahault 1888; Correns 1889; Kiseleva 1930; Fiore et al. 2007; Sant'Anna et al. 2010; Komárková et al. 2013; McGregor & Sendall 2017a, b). The genus *Scytonema* Bornet & Flahault was initially created for filamentous cyanobacteria with solitary filaments or form of clusters as prostrate with obligatory geminate, entangled filaments, false branching, intercalary heterocytes, and vegetative cells that are mostly green, olive–green, blue–green or yellowish (Komárek 2013; Komárek & Johansen 2015). *Scytonema* includes about 127 described species, mostly known from tropical and subtropical regions (Komárek et al. 2013; McGregor 2018). Currently, increasing evidence obtained mainly from molecular phylogeny, has shown that the taxonomy of the genus *Scytonema* is divergent. Phylogenetically, relationships of species within the genus *Scytonema* are not clear, indicating a polyphyletic genus. Therefore, a taxonomic revision of the genus *Scytonema* had been extensively undertaken leadingto the definition of the '*Scytonema* sensu stricto' clade, with the type species *Scytonema hofmanii* of the genus *Scytonema* used to settle taxonomic problems (Komárek et al. 2013). Several novel genera and species have been separated from the genus *Scytonema* on the basis of molecular comparison using 16S rRNA sequences, ITS secondary structures, and phylogenetic analyses of *Scytonema*–like species belonging to the Scytonemataceae (Singh et al. 2016, 2017; Saraf et al. 2018; Sendall & McGregor 2018). However, few 16S rRNA sequences of *Scytonema* strains within the *Scytonema* sensu stricto clade have been published and information from polyphasic studies of *Scytonema* is relatively poor and requires further investigation.

In this study, two novel strains were isolated from a wet soil sample from the Khek River in Phitsanulok Province in the lower northern part of Thailand. A polyphasic approach was used to characterize these strains by examining morphological features, phylogenetic analyses based on 16S rRNA, rbcLX, and nifH sequences. Secondary structures of the 16S–23S rRNA internal transcribed spacer (ITS) were also investigated. These strains displayed *Scytonema*–like morphology, but, based on morphological and phylogenetic analyses, they were distinctly separated from the type species *Scytonema hofmanii* within the *Scytonema* sensu strico clade. We found that our strains produced the odoriferous compound, geosmin, based on olfactory and demonstration of the geosmin synthase (geoA) gene. Therefore, the novel *Scytonema* species, *S. foetidum*, is hereby proposed.

MATERIALS AND METHODS

Cyanobacterial isolation and cultivation. A wet soil sample was collected from the Khek River (16°51'09.8"N, 100°36'43.9"E) in the lower northern part of Thailand during April 2019 (summer season). Cyanobacteria isolation was conducted by the traditional microbiological method using micromanipulation of single filaments onto modified solid CT/2 medium (Yamamoto 2011), with 0.4% agarose. The isolated cyanobacteria were also treated with 355 mM of cycloheximide to remove contaminating eukaryotes. *Scytonema*–like filaments were picked after an extended growth period (more than one month) and isolated into pure culture. Two clonal strains were successfully established and maintained in modified liquid CT/2 medium under a light cycle of 12:12 (light:dark period) at 25 °C. Light intensity during the light period was 40 μmol photons $m^{-2}.s^{-1}$. The strains were maintained in the Naresuan University Algae and Cyanobacteria Collection (NUACC), Thailand, and coded as NUACC05 and NUACC06.

Morphological characterization. Morphological observation and morphometric measurements of the novel strains were conducted using a light microscope (BX63, Olympus, Tokyo) equipped with high–resolution Nomarski DIC optics and an Olympus DP74 digital camera. Cultures were regularly inspected for morphological changes throughout the life–cycle stages for more than one month. The specimens were preserved (final concentration of 4% formaldehyde) and measured for morphometric characters that play an important role in the taxonomy of cyanobacteria such as the length (L) and width (W) of filament, vegetative, and heterocyte cells using AxioVision LE64 V 4.9.1.0 software. Morphometric information was based on 50–100 measurements for each parameter and are expressed as minimum, average and maximum values in the taxonomic description.

DNA extraction, PCR amplification and sequencing. A lithium acetate–sodium dodecyl sulfate (LiOAc–SDS) DNA extraction method was used to extract genomic DNA from the isolated strains. Briefly, 1 ml of unialgal culture in the exponential phrase (*ca*. 14 days) was harvested by centrifugation for 1 min at 3,000 rpm, and then rinsed with sterile deionized water three times. The cell pellet was resuspended in 100 μl of 200 mM LiOAc 1% SDS solution, and incubated for 15 min at room temperature. Then, a volume of 300 μl of 95% ethanol was added for DNA precipitation. After mixing briefly, the sample was centrifuged at 14,000 rpm for 3 min and the supernatant was discarded. The DNA pellet was rinsed with 300 μl of 70% ethanol and subsequently centrifuged at 14,000 rpm for 10 min. The DNA pellet was air dried at room temperate and then suspended in 100 μl of Tris–EDTA to use as a PCR template.

Segments of the 16S rRNA (nt 27 to end) and the 16S–23S rRNA internal transcribed spacer (ITS) region were amplified using primer sets 27F/23S30R and 322F/340R, respectively, following a previous study (Tawong et al. 2019). To increase

the molecular evidence, rbcLX and nifH gene segments were also amplified. For the rbcLX gene segments (ca. 900 bp), the CX/CW primer set designed by Rudi et al. (1998) was used. The nifH gene segment (ca. 400 bp) was obtained by amplification using the cyanobacterial selective CNF/CNR primer set (Olson et al., 1998). During cultivation, an odiferous smell was observed associated with the strains. Therefore, screening for the geosmin (geoA) and 2–methylisoborneol (MIB) synthase genes was performed using primer sets geo78F/geo982R and MIB3313F/MI4226b, respectively (Suurnäkki et al. 2015). The PCR reaction, with a total volume of 25 μl, contained: 11.5 μl of sterile water, 0.5 μl of each primer (0.01 mM concentration), 12.5 μl of OnePCR Ultra Supermix w Fluorescent Dye Master Mix (Bio–Helix, Keelung, Taiwan), and 3 μl of template DNA (20 ng.μl⁻¹). PCR was performed in a MyCycler™ Thermal Cycler (Bio–Rad, Hercules, CA, USA) and the amplification program was carried out as follows: one cycle of 2 min at 94 °C; 30 cycles of 30s at 94 °C, 30s at 50 °C, and 2 min at 72 °C and then a final 5 min elongation step at 72 °C. The PCR products were purified using PureDireX PCR Clean–Up & Gel Extraction Kit (Bio–Helix, Keelung, Taiwan) following the manufacturer's instruction. The purified PCR products were then sequenced using an ABI PRISM BigDye Terminator V3.1 Kit (Applied Biosystems, , Foster City, CA, USA). All primer sets used in the amplification and additional primers CYA106F, CYA359F, 809R, 740F, and 1494Rc were used for 16S rRNA sequencing. The nucleotide sequences of each primer were assembled into contigs with 100% overlapping regions, and then the consensus sequence obtained was used for molecular analyses. All consensus sequences obtained in this study were submitted to GenBank under accession numbers LC633739–LC633743 for 16S rRNA sequences, LC633744–LC633747 for 16S–23S rRNA ITS sequences, LC633750– LC633751 for nifH gene sequences, LC633748– LC633749 for rbcLX gene sequences, and LC633737– LC633738 for geoA gene sequences.

Phylogenetic analyses, sequence analysis, and ITS folding. All obtained sequences of each gene investigated in this study were aligned separately with reference sequences from GenBank using MUSCLE (Edgar 2004) in Unipro UGENE v.39.0 (Okonechnikov et al. 2012). For the 16S rRNA sequences, short sequences (<700 bp) were excluded from analyses (Yarza et al. 2014). Phylogenetic trees were constructed using neighbor–joining (NJ), maximum likelihood (ML), and Bayesian inference (BI) approaches. To explore the sequence evolution model the fitted dataset based on the Akaike information criterion (AIC), the MrModeltest 2.4 (Nylander 2004) was performed. The best–fit model selected for the ML and BI analyses of the 16S rRNA, rbcLX, nifH, and geoA dataset was GTR+I+G. The NJ algorithms using a p–distant model were run via MEGA–X software V.10.0.5 (Kumar et al. 2018), the ML analysis was conducted using PhyML 3.0. (Guindon et al. 2010), and BI was analyzed with MrBayes 3.2.2 (Ronquist et al. 2012). Bootstrap analyses of 1,000 replicates for the NJ tree and 100 replicates for the ML tree were performed. The BI analyses were performed using four runs of four chains, sampling from the chain every 100 generations. The number of generations used in these analyses were 6.0×10^6 generations for 16S rRNA and nifH alignments and 2.5×10^6 generations for rbcLX and geoA alignments. After the standard deviation values of the two runs dipped below 0.01, the number of trees discarded as burn–in value were 4.2×10^4 trees for the 16S rRNA alignment, 1.4×10^4 trees for rbcLX alignment, 4.5×10^4 trees for nifH alignment, and 4.0×10^3 trees for geoA alignment. The rest was to calculate the posterior probabilities (pp) of

branches. *Microcystis aeruginosa* MK10.10 (FN678905) was used as an outgroup for the 16S rRNA phylogenetic trees, *Synechococcus elongatus* strain PCC6301 (AP008231) was an outgroup for the rbcLX trees, and *Azotobacter vinelandii* (M20568) was an outgroup for the nifH trees, whereas the sequences described by Suurnäkki et al. (2015) were used as the outgroup for the geoA trees.

The genetic (p) distance value was calculated using MEGA–X software V.10.0.5 and used to assess the sequence similarity percentages as 100× (1–p) among the sequences. Secondary structures of the 16S–23S rRNA ITS region from our strains were compared with closely related taxa presenting in the 16S rRNA phylogenic interpretations. The tRNA sequences were determined with tRNAscan–SE 1.21 (Lowe & Eddy 1997), while the 16S–23S rRNA ITS secondary structures of D1–D1′, Box–B, V2 and V3 helices were investigated using RNA structure version 6.0.1 (Mathews Lab 2018).

Results

Species description

Scytonema foetidum W. Tawong, P. Pongcharoen et T. Nishimura sp. nov. (Figs 1A–U)
Description: Blue–green mat–like biofilm; isopolar filament with 3.94–(5.43)–9.45 μm in width, cylindrical, continually widened toward the basal zone, single or binary false branching, sometime single false branching present after loop–like lateral formation, filament densely arranged; sheath thin, smooth, sometime rough, distinct in texture colorless and rarely up to brownish; sheath present throughout the length of trichome; trichome cylindrical, constricted or unconstricted at cross–walls, less or absent constrictions in younger filaments but distinct in older filaments, basal parts widened, terminal parts of branches slightly cylindrical, with rounded–tapering apical ends; vegetative cell cylindrical to disc–like shape with 2.38–(4.49)–12.77 μm in length and 2.85–(4.27)– 0.70 μm in width, with granular content, young cells mostly longer than wide, whereas old cells were shorter than width, blue–green in color; apical cell conically rounded without calyptra and less presence of sheath covering; heterocytes intercalary, cylindrical to discoid shape; single or in pairs; length ranging from 4.20–(7.39)–12.74 μm, whereas the width ranging from 3.84–(5.24)–7.62 μm; reproduction by homogonia; akinetes not present. D1–D1′ helix of the 16S–23S rRNA ITS region with 99 nucleotide long, V2 helix with 67 nucleotides, Box–B with 31 nucleotides, V3 helix with 88 nucleotides with five internal loops; both tRNA coding isoleucine and alanine were present.

Designated holotype: A formaldehyde–fixed specimen of strain NUACC06 was deposited at the Queen Sirikit Botanic Garden Herbarium (QBG), the Botanical Garden Organization, Chiang Mai, Thailand under the designation as QBG No. 131045.
Reference strain: A representative strain was deposited

at the Naresuan University Algae and Cyanobacteria Collection (NUACC), Faculty of Agricultural Nature Resources and Environment, Naresuan University, Phitsanulok, Thailand, under the designation NUACC06.
Type locality: Found in wet soil on the bank of the Khek River, Phitsanulok, the lower northern part of Thailand (16°51'09.8"N, 100°36'43.9"E).
Etymology: From the Latin "*foetidum*"; this species produces an earth/musty odor.
Habitat: A wet soil sample was collected from the Khek River, Phitsanulok, during April, which is the summer season of Thailand.
Gene Sequences: LC633740 and LC633742 for the 16S rRNA region, LC633749 for the rbcLX gene, LC633751 for the nifH gene, LC633745 and LC633747 for the 16S–23S rRNA ITS region, and   LC633737 for the geoA gene.

Differentiation from other species

Under light microscopy, the morphological character of *S. foetidum* was similar to the description of *S. hofmanii* in colonial and cellular shapes except for smaller width of the filaments and vegetative cell sizes, as well as the conically rounded apical cell. *Scytonema foetidum* also presented a distinct sheath. Furthermore, the loop–like lateral formation sometimes became a single false branch. The molecular phylogeny based on 16S rRNA, rbcLX, and nifH sequences also showed that this species had a unique position in relation to *S. hofmanii* strain PCC7110, the type strain of the genus *Scytonema*. Moreover, low similarity values in 16S rRNA and the 16S–23S rRNA ITS region sequences of *S. foetidum* to those of closely reated *Scytonema* taxa and significant differences in length and secondary structures of the 16S–23S rRNA ITS region with two operon types (with and without tRNAs in the ITS region), support the separation of *S. foetidum* as a new species in the genus *Scytonema*. Furthermore, the novel species could also produce the odoriferous compound, geosmin.

Morphological analyses

Morphologies of *S. foetidum* (strains NUACC05 and NUACC06) were compared with other known *Scytonema* species (Table 1). In the culture period, *S. foetidum* strains NUACC05 and NUACC06 showed moderate growth as a bluish–green mat–like biofilm attached to the tube surface (Fig. 1a). Light microscopy revealed that both strains possessed some morphological characters in common with the genus *Scytonema*. Filaments were isopolar, rarely heteropolar, free or in fascicles, cylindrical, slightly widened toward the basal zone, densely arranged, with single and binary false branching, with pale–greenor yellow–brown in older filaments (Figs 1b–h). The sheath was distinctly textured thin, smooth, sometimes rough, colorless and rarely yellow–brown (Figs 1b–d, f). The presence of the sheath was visible throughout the length of the trichome (Figs 1c–d). False branching was exhibited as single or binary (Figs 2e–k).

Branched false ramification originated after trichome detachment from the formation of necridia cells, typically between two adjacent heterocytes (Figs 1f, j–k), and sometimes from heterocyte cells resembling species in the genus *Tolypothrix* (Figs 1e, i). A loop–like lateral formation was also present and later the tops of the loop ruptured to frequently become binary false branching (Figs 1e–f). Moreover, the development of a single false branching was sometimes found after breaking the tops of the loop–like lateral part (Fig. 1h). This characteristic has not been reported in other *Scytonema* species. The middle part of the trichome was cylindrical, the basal parts slightly widened, and the terminal parts slightly cylindrical, with rounded–tapering end (Figs 1b–e, l–q). Constrictions between cells were fewer or absent in the younger filaments, and became distinct in the older filaments (Figs 1b–e, g, l–s). Vegetative cells were cylindrical to disc–like shaped, with granule content and blue–green (Figs 1b–d, k, r–s). Apical cells were conically rounded without calyptra (Figs 1l–q), resembling the characteristics of *S. stuposum* and *S. hyalinum*. Vegetative cells in terminal to middle trichome (young or developing cells) were cylindrical to square, mostly longer than wide (Figs 1c–d, l–q), whereas basal or older cells were rectangle to barrel–shaped, and wider than long (Figs 1b, e, g, r–s). Heterocytes were intercalary, variously shaped, generally rectangular to square in young cells, rectangular to discoid in old cells, sometimes octagonal, single or in pairs (Figs 1c–d, r–s). Reproduction occurred by the production of hormogonia, which developed at the ends of branches or between necridia cells and detached from the sheaths (Figs 1t–u). Akinetes were not observed in the cultured material.

Molecular phylogenetic and sequences analyses

The 16S rRNA, rbcLX, and nifH genes were successfully amplified and sequenced from *S. foetidum* strains (NUACC05 and NUACC06) to assist in species identification. The 16S rRNA sequences of the two *S. foetidum* strains showed 100 % sequence similarity among the replicated sequences within each strain. The phylogenetic reconstruction of BI, ML, and NJ methods based on the 16S rRNA sequences (1,428 bp) from 117 cyanobacteria taxa revealed that strains identified as *Scytonema* formed a polyphyletic clade (Fig. 2). Furthermore, results indicated that the *Scytonema* sensu stricto formed a distinct clade, which was a sister to the genera *Ewania*/*Iphinoe*/*Brasilonema*. In the branch of the *Scytonema* sensu stricto clade, 11 subclades (S1–S11) were identified (Fig. 2). The ML trees revealed that three sequences of *S. hofmanii* PCC7110 (AM709637, AF132781, and NR_112180; from a limestone cave in Bermuda) as the type strain of *Scytonema*, grouped together with *Scytonema* sp. FM05–MK45 (KY418179; from a tropical greenhouse in the Czech Republic) (BI=1.00, ML=93, and NJ=100) as named by subclade S6. Interestingly, the 16S rRNA phylogeny revealed that *S. foetidum* strains (NUACC05 and NUACC06) were grouped into a unique
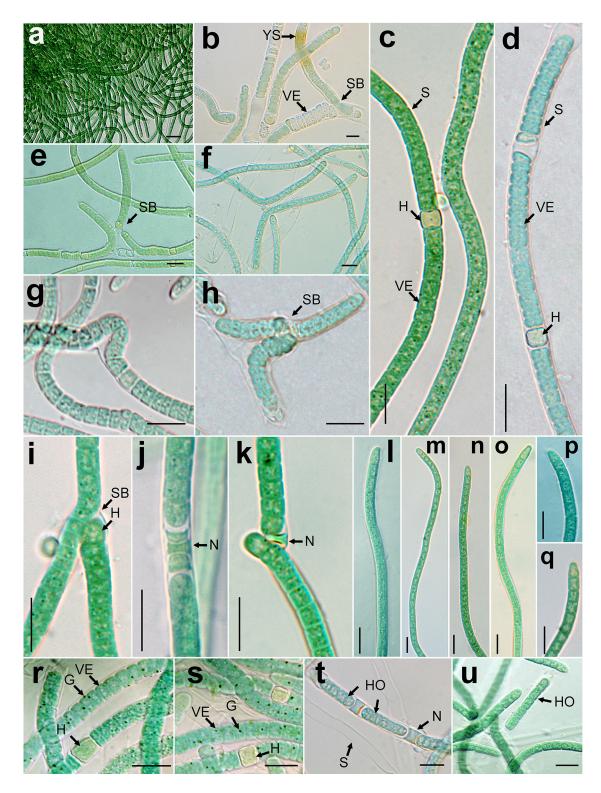
Fig. 1. Morphological details of *Scytonema foetidum* strain NUACC06: (a) densely fasciculate filament; (b) old filament showing disc–like vegetative cells and yellow–brown sheath; (c–d) visible sheath presenting though filament and cylindrical trichome with intercalary heterocyte cells; (e–f) the single and binary false branching; (g) loop–like lateral formation; (h–i) single false branch growing from the lateral–like loop and heterocyte cell; (j) formation of necridia cells; (k) initiation of branching after disintegrating of sheath at the site of a necridia cell; (l–q) developing filament with the apical end showing slightly conical–round shape; (r–s) trichome presenting various shapes of vegetative cells containing stock granules with distinct constriction at the cell wall; (t) homogonia formation between the necridia cells; (U) a releasing homogonia. Designations: (VE) vegetative cell; (YS) yellow–brown sheath; (SB) single branching; (H) heterocyte cell; (N) necridia cell; (G) stock granules; (HO) homogonia. Scale bar 20 μm (a); 10 μm (b–u).

Table 1. Comparison of morphological characteristics of *Scytonema foetidum* sp. nov. and closely related *Scytonema* taxa. This table was adapted from SARAF et al. (2018).

	S. pachmarhiense	*S. bilaspurense*	*S. singhii*	*S. hofmanii*	*S. foetidum*	*S. crispum*	*S. stuposum*	*S. hyalinum*
Filament	Isopolar filaments with solitary and frequent binary false branching	Isopolar filaments with solitary false branching	Isopolar filaments with solitary false branching	Isopolar filaments with geminate or solitary false branching; W: 7–12 μm	Isopolar filaments; densely arranged; widen at the basal part; single or binary false branching; W: 3.94–(5.43)–9.45 μm	Short to long isopolar filaments; solitary or binary false branching	Short; densely arranged; single or double false branching	Densely entangled; single or double false branched
Vegetative cell	±Cylindrical; wider than length; terminal cell have curved ends L: 4.9–7.6 μm; W: 8.6–9.1 μm	±Cylindrical; wider than length; terminal cell have curved ends L: 5.5–11.6 μm; W: 5.6–9.7 μm	±Cylindrical; wider than length; terminal cell have curved ends L: 3.6–6.9 μm; W: 5.6–6.9 μm	±Cylindrical; slightly widened at ends; Older cells ± isodiametric; W: 5–10 μm	Cylindrical to disc-like; sometime longer than wide in the younger cell; wider than long in the older cell; terminal cell slightly tapering shaped L: 2.38–(4.49)–12.77 μm; W: 2.85–(4.27)–10.70 μm	Barrel shaped to disc-like; slightly narrowed at the ends L: 2–10 μm; W: 10–17 μm	Cylindrical to disc-like; wider; terminal cell rounded or conical L: 2–6 μm; W: 8–18 μm	Barrel to cylindrical shaped; terminal cell have conical ends L: 4.6–8 μm; W: ± 9 μm
Heterocyte	Solitary; long; cylindrical; with concave and convex ends L: 7.8–15.2 μm; W: 8.7–9.7 μm	Solitary; square to cylindrical; never have rounded ends L: 3.1–4.7 μm; W: 6.6–8.8 μm	Solitary; square to cylindrical; never have rounded ends L: 4.8–13.1 μm; W: 5.2–6.9 μm	Solitary or in pairs; cylindrical with rounded ends or ellipsoid W: 5–10 μm	Solitary or in pairs; cylindrical to discoid; L: 4.2–(7.39)–12.74 μm; W: 3.84–(5.24)–7.62 μm	Solitary; flattened; different shapes; yellow-green colored W: 10–17 μm	Single or in pairs; cylindrical beige to yellow colored L: 4–10 μm; W: 10–15 μm	Cylindrical with rounded ends; shorter than wide L: 5–18 μm; W: 6–12 μm
Sheath	Thin and narrow sheath; present throughout the trichome; colourless	Thin and narrow sheath; present throughout the trichome; colourless	Thin and narrow sheath; present throughout the trichome: colourless	Thin and narrow, ±slightly lamellated; colourless or yellow up to yellow-brown on wet wood.	Thin and narrow sheath: present throughout the trichome; colourless or yellow in the older filament	Thick; colourless-yellow; orange-brownish; slightly lamellated; closed at ends	Thin up to 4 μm wide; unstructured; colourless; closed at trichome ends	Firm and thin; slight lamellated; colourless; yellow-brown when old less on wet soil
Habitat	Freshwater	Freshwater	Freshwater	Wet walls; soils; stones	Wet soils	Aquatic	Wet soils; among mosses; on rocks	Stony substrates

Fig. 2. Maximum likelihood tree based on the phylogenetic relationship of the 16S rRNA sequences (1,428 base pairs) of two *Scytonema foetidum* strains (five sequnces) and other cyanobacterial taxa (123 sequences). Studied *Scytonema foetidum* strains are in bold. *Microcystis aeruginosa* MK10.10 was used as the outgroup. Posterior probabilities from BI method and bootstrap support from ML and NJ methods at and above 0.50 and 50% are only indicated at nodes and the lower value is shown as a hyphen (–). S1–S11 showing at node present the number of subclades within the *Scytonema* sensu stricto clade. Clades of related taxa distant from *Scytonema* were collapsed. (T) represents the type strain of the genus *Scytonema*. Asterisks at the nodes equal 0.99–1.00 posterior probabilities or 99–100% bootstrap support values. Bold horizontal lines show clades supported by at least 0.75 of BI posterior probabilities and 75% of ML and NJ bootstrap values. Scale bar indicates the number of nucleotide substitutions per site.

clade (subclade S9) with robustly supported values from BI (1.00), ML (100), and NJ (100) approaches (Fig. 2). This unique clade was positioned between the subclades S8 and S10/S11 (BI=1.00, ML=83, and NJ=67). Based on the comparison of 16S rRNA sequences similarity values, the *Scytonema* sensu stricto clade was separate, with closely related genera including *Ewamiania* (93.0%), *Iphinoe* (92.8%), and *Brasilonema* (93.7%) (data not shown). A comparison based on the 16S rRNA

sequences between *S. foetidum* (subclade S9) and the most phylogenetically related taxa showed maximum similarities at 98.4% with uncultured cyanobacteria strain TG32 (JQ769542, subclade S8), 97.3% with *Scytonema* sp. IAM M–262 (AB093483, subclade S10), and 97.9% with *Scytonema* sp. U–3–3 (AY069954, subclade S11) (Table 2). Furthermore, *S. foetidum* also distantly shared 16S rRNA sequence similarity (95.6%) when compared with *S. hofmanii* PCC7110 (subclade S6), the type strain
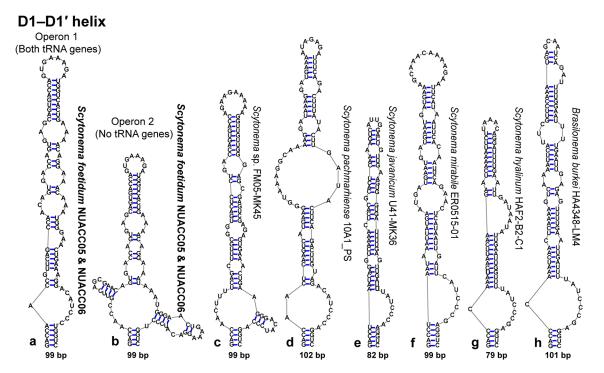
D1–D1′ helix

Fig. 3. Hypothetical secondary structures of the D1–D1′ helix of the 16S–23S rRNA ITS region in *Scytonema foetidum* sp. nov., and closely related taxa for which the sequence data are available. Nucleotide lengths are shown below each structure of strain investigated in this study.
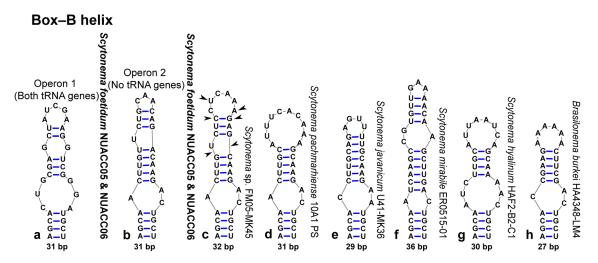
Box–B helix

Fig. 4. Predicted secondary structure of the Box–B helix of the 16S–23S rRNA ITS region in *Scytonema foetidum* sp. nov., and closely related taxa for which the sequence data are available. Arrows on (c) indicate variable sites and insertion/deletions of base pairs compared with *S. foetidum*. Nucleotide lengths are shown below each structure of strain investigated in this study.

of genus *Scytonema* (Table 2).

The rbcLX gene phylogenetic trees showed that the *Scytonema* strains also formed a polyphyletic clade. Two *S. foetidum* strains (NUACC05 and NUACC06) formed a sister clade (BI=1.00, ML=100, and NJ=98) to a close clade containing *S. hofmanii* PCC7110 (ANNX02) and *Scytonema* sp. FM05–MK45 (KY417065) with strongly supported values from BI (1.00), ML (99), and NJ (98) analyses (Fig. S1a). Analysis based on the rbcLX sequence similarity comparison with closely related taxa showed that two strains of *S. foetidum* shared 93.0% similarity with *S. hofmanii* PCC7110 and 93.3% with *Scytonema*

sp. FM05–MK45 (Table S1).

The nifH gene phylogenetic trees obtained from BI, ML, and NJ analyses revealed that two *S. foetidum* strains formed a sister clade (BI=1.00, ML=92, and NJ=61) to *S. hofmanii* PCC7110 (AY768414), whereas a cluster of *Scytonema* sp. NC–4B, DC–A, and FGP–7A (DQ531694, DQ531695, and DQ531669) formed the basal taxon of the branch (BI=1.00, ML=92, and NJ=71) (Fig. S1b). The maximum similarity value based on the nifH gene sequences showed that *S. foetidum* strains shared 91.4% similarity with *S. hofmanii* PCC7110 (AY768414) (Table S2).

Comparative analysis of the 16S–23S rRNA ITS region
Since 16S–23S rRNA ITS region data for the type strain of *Scytonema* (*S. hofmanii* PCC7110) has not been determinedyet, the available ITS region sequences of *Scytonema* sp. FM05–MK45, which is a closely related strain to *S. hofmanii* PCC7110, and phylogenetically related strains were used for secondary structure comparisons. In this study, the obtained 16S–23S rRNA ITS sequence was identical amongst the two *S. foetidum* strains, and showed that *S. foetidum* has two ribosomal operon types; the first operon type (operon type 1) with both tRNA (Ile and Ala) genes in this region, and the second operon type (operon type 2) that lacked tRNA genes. The basal stem of the D1–D1′ helix of all strains tested was the most conserved structure with four base pairs (5′–GACC–GGUC–3′) (Figs 3a–h). The D1–D1′ helix of *S. foetidum* was extensive with 99 nucleotides in both operons, similar to those of *Scytonema* sp. FM05–MK45 and *Scytonema* cf. *mirable* ER0515_01 (Figs 3a–c). However, the folded secondary structures of the D1–D1′ helix in both operons from *S. foetidum* had considerably different lengths and structures from the closely related species of the genera *Scytonema* or *Brasilonema* (Figs 3a–h). Among the operon types 1 and 2 of *S. foetidum*, the D1–D1′ helix structures were very different (Figs 3a–b). The D1–D1′ helix structures in operon type 1 (Fig. 3a) mostly resembled that of *Brasilonema burkei* HA4348–LM4 (Fig. 3h), but differed in length and structure of the terminal part. The D1–D1′ helix region in operon type 2 of the *S. foetidum* strains showed a multiloop with small lateral hairpin loops

on each side (5′ and 3′), resembling the D1–D1′ helix structure of *Scytonema* sp. FM05–MK45 which has a multiloop with a unilateral loop at the 3′ side (Figs 3c). The Box–B helices were also more variable in terms of length and sequence between *S. foetidum* and all other taxa compared (Figs 4a–h). The basal part of the Box–B helix was a highly conserved region in all strains investigated with four base pairs (5′–AGCA–UGCU–3′). Furthermore, the Box–B helix structure of operon type 1 presented a unique structure when compared with other closely related *Scytonema* taxa, whereas that of operon type 2 was mostly similar to the structure of *Scytonema* sp. FM05–MK45 which was only different at the terminal loop. The V2 helix region of taxa within the *Scytonema sensu stricto* clade has not been determined yet. However, V2 helix region of *S. foetidum* was only found in operon type 1 with a length of 67 bp which was shorter than that of all other taxa compared (Figs 5a–c). The V3 helix was also present as a variable long helix ranging from 67 to 88 bp. The V3 helix structures of *S. foetidum* in operon types 1 and 2 were identical and quite distinct from those in all other taxa compared, with the basal stem containing a 3–bp helix followed by five bilateral bulges, and the terminal loop consisted of seven nucleoside bases (5′–AGAAAAA–3′) (Figs 5d–i).

Mostly, the available 16S–23S rRNA ITS sequences of *Scytonema* taxa in the *Scytonema* sensu stricto clade lacked tRNAs (named as operon type 2 in this study). Thus, these sequences were used to compare the percent similarity. Genetic distance comparison based on the ITS region lacking tRNAs showed that *S. foetidum* had low
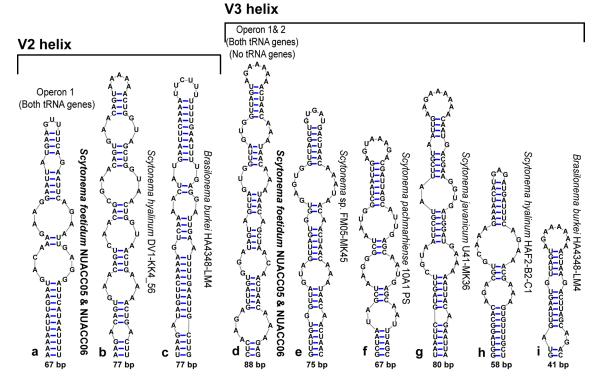

Fig. 5. Secondary structures of V2 and V3 helices of the 16S–23S rRNA ITS region in *Scytonema foetidum* sp. nov. and closely related taxa for which the sequence data are available. Nucleotide lengths are shown below each structure of strain investigated in this study.

Table 2 Comparison of percent similarity values based on 16S rRNA sequences (1,428 bp) among selected taxa phylogenetically related to *Scytonema foetidum* sp. nov. The *S. foetidum* strains and its similarity values are shown in bold letter.

Strain	1	2	3	4	5	6	7	8	9	10	11	12	13	14	15	16
1 *Scytonema foetidum* NUACC06	**100**															
2 *Scytonema foetidum* NUACC05	**98.4**	**100**														
3 Uncultured bacterium clone TG-32	98.4	98.4	100													
4 *Scytonema* sp. IAM M-262	97.3	97.3	97.7	100												
5 *Scytonema* sp. U-3-3	97.9	97.9	97.1	97.7	100											
6 *Scytonema singhii* 1F-PS	97.0	97.0	97.3	96.8	95.9	100										
7 *Scytonema bilaspurense* 10C-PS	96.9	96.9	97.2	96.7	95.8	99.9	100									
8 *Scytonema* sp. 6SS	96.7	96.7	97.2	96.9	96.7	98.0	97.9	100								
9 *Scytonema* sp. FM05-MK45	95.9	95.9	95.8	95.0	95.6	96.9	96.8	96.6	100							
10 *Scytonema hofmanii* PCC7110	95.6	95.6	95.4	94.4	94.8	96.9	96.7	96.5	98.9	100						
11 *Scytonema pachmarhiense* 10A1_PS	95.3	95.3	95.5	95.3	95.0	95.8	95.7	95.8	93.9	93.7	100					
12 Uncultured bacterium clone HL627	95.3	95.3	95.5	94.6	94.7	96.6	96.5	96.3	96.9	96.9	94.0	100				
13 Uncultured bacterium clone YF407	94.6	94.6	94.8	93.9	94.3	95.9	95.8	96.1	96.3	96.4	93.2	98.3	100			
14 *Scytonema hyalinum* HAF2.B2.c1	92.8	92.8	92.9	92.0	92.7	93.8	93.7	93.8	94.9	94.7	93.0	94.0	93.0	100		
15 *Scytonema javanicum* U41-MK36	92.7	92.7	92.7	93.0	92.2	94.3	94.2	94.6	93.9	93.9	93.8	94.0	94.3	94.0	100	
16 *Scytonema* cf. *mirabile* ER0515.01	92.2	92.2	93.5	93.1	92.5	94.6	94.5	94.7	93.5	93.4	92.8	93.9	93.1	92.9	93.3	100

similarity with *Scytonema* sp. FM05–MK45 (83.0%), *Scyonema* cf. *mirabile* ER0515.01 (74.8%), *Scytonema pachmarhiense* 10A1_PS (69.9%), and *Scytonema javanicum* U41–MK36 (64.6%) (Table 3).

Screening for the odor compound

During cultivation, two *S. foetidum* strains (NUACC05 and NUACC06) produced an odoriferous smell based on olfactory screening. Thus, partial geosmin (geoA) and MIB synthase genes were investigated from these two strains. Results of the PCR amplification revealed that segments of the geoA gene were found in the two *S. foetidum* strains. Phylogenetic trees based on 885 nucleotides of the geoA gene also indicated that two *S. foetidum* strains formed a sister clade to *Scytonema* sp. CHAB3651 (BI=1.00, ML=98, and NJ=100) and followed a basal clade containing two strains of *Neowollea manoromensis* NUACC12 (LC474827) and NUACC15 (LC474826) (Fig. S2). The sequenced geoA gene segments of *S. foetidum* shared maximum similarity (88.3 %) with *Scytonema* sp. CHAB3651 from China (data not shown).

DISCUSSION

Cyanobacterial systematics have been extensively modified after the acceptance of polyphasic approaches (KOMÁREK et al. 2014) that allowed higher confidence in assertions regarding the relationships between members within the genus *Scytonema* leading to considerable taxonomic revisions (KOMÁREK et al. 2014; JOHANSEN et al. 2017; SARAF et al. 2018). Modern criteria for the judgment of species genotype of *Scytonema* strains were established as follows 1) two strains were advocated as different species, if they shared a 16S rRNA identity of <98.7% in either operon type, 2) if the strain showed a unique phylogenetic position separating it from the nearest sister clade it was considered to be a separated species, and 3) morphologically different species were accepted based on phenotypic traits even though molecular evidence supporting their separation was not distinct (JOHANSEN et al. 2017). In this study, a novel *Scytonema* species, *S. foetidum*, was distinguished from known *Scytonema* taxa despite presenting only subtle morphological variation when compared to previously described *Scytonema* species (Table1).

Table 3 Percent similarity values among the ITS region in comparison with orthologous operon lacking tRNAs. Comparisons between *S. foetidum* and members within the *Scytonema sensu stricto* clade which the 16S–23S rRNA ITS region sequences are available. The *S. foetidum* strains and its similarity values are shown in bold letter.

	Strain	1	2	3	4	5	6
1	***Scytonema foetidum* NUACC06**						
2	*Scytonema* sp. FM05-MK45	**83.0**					
3	*Scyonema* cf. *mirabile* ER0515.01	**74.8**	76.4				
4	*Scytonema pachmarhiense* 10A1_PS	**69.9**	72.8	71.5			
5	*Scytonema javanicum* U41-MK36	**64.6**	71.5	67.9	63.0		
6	*Scytonema hyalinum* HAF2.B2.C1	**63.4**	68.3	70.3	66.7	70.3	

Two *S. foetidum* strains NUACC05 and NUACC06 shared morphological characteristics with members of the genus *Scytonema* including binary false branching, a cylindrical shaped trichome, and mostly surrounded by a sheath (KOMÁREK 2013; MCGREGOR 2018). However, the two novel strains do not fully meet the morphological criteria as compared with phylogenetically related *Scytonema* taxa in the *Scytonema sensu stricto* clade and the other *Scytonema* clusters, since they possessed a small width filament and vegetative cell, and the presence of single false branching after loop–like lateral formations (Table 1). Characteristics such as sheath type and trichome termination could promote morphological circumscription within the genus *Scytonema* (KOMÁREK 2013; SIGH et al. 2016; SINGH et al. 2017; SARAF et al. 2018). The presence of a distinctly textured thin sheath, which could be visible throughout the length of the trichome, and a slightly tapering apical cell were also important distinguishing features that differentiated *S. foetidum* from the type species of *Scytonema*, *S. hofmanii* (Table 1). Morphological examination results indicated that *S. foetidum* was separate from other known *Scytonema* species.

It is known that variation of morphological traits may be triggered by environmental factors resulting from culture or natural condition (CASAMATTA & VIS 2004; PERKERSON et al. 2011; MCGREGOR & SENDALL 2021). Therefore, molecular differences are the most powerful evidence for identifying and separating species and genera across the cyanobacteria (JOHANSEN & CASAMATTA 2005). The results of the 16S rRNA sequences phylogenetic analysis were consistent with previously published phylogenies, indicating that the strains identified as *Scytonema* form a polyphyletic assemblage (KOMÁRKOVÁ et al. 2013; SIGH et al. 2017; MCGREGOR & SENDALL, 2017a,b; JOHANSEN et al. 2017; SARAF et al. 2018). JOHANSEN et al. (2017) reported multiple operons in the 16S rRNA from several *S. hyalinum* strains using clone libraries (named as *S. hyalinum* type 1 and type 2 in the present study), this feature did not appear uniquely distinct in the *Scytonema* sensu stricto clade containing our strains, corresponding to the previous study of SARAF et al. (2018). The two strains of *S. foetidum* formed a distinct

monophyletic lineage, separated from other subclades in the *Scytonema* sensu stricto clade, in both the 16S rRNA, rbcLX, and nifH gene phylogenetic reconstructions with good statistical support in all analyses performed (BI, ML, and NJ methods). Furthermore, new analyses of our 16S rRNA sequence trees revealed divergence within the *Scytonema* sensu stricto clade, including uncultured and cultivated microorganisms. Unfortunately, some uncultured strains (e.g., subclades S5 and S8) have not been investigated for their morphological features or other taxonomic criteria. Such is the case for the vast number of *Scytonema*–morphospecies which have yet to be sequenced (i.e. *S. santannae* from the Atlantic rainforest in southeastern Brazil; HENTSCHKE & KOMÁREK 2014), particularly those in tropical and subtropical regions where biodiversity has been in historically underestimated. We suggest that more representative strains clustering with the uncultured strain subclades should be collected and investigated to confirm divergence within the *Scytonema* sensu stricto clade.

According to the literature, a 95% similarity value for the 16S rRNA sequences is the threshold of distinction for certain cyanobacterial genera, and >98.7% is used to identify to the same cyanobacterial species (STACKEBRANDT & EBERS 2006; YARZA et al. 2014; KIM et al. 2014). Based on comparison of the 16S rRNA sequence, *S. foetidum* exhibited a low percentage of similarity (95.6 %) to the type strain of *S. hofmanii* PCC7110, and also showed a large genetic divergence from other known *Scytonema* species within the *Scytonema sensu stricto* clade (92.2–98.4%) (Table 2). Furthermore, the rbcLX and nifH sequence similarities from the two strains of *S. foetidum* were also low (<93%) compared to known strains in *Scytonema* sensu stricto clade (Tables S2 and S3). Nonetheless, modern systematics approaches should use other tools of evolutionary relationship reconstruction (i.e. the 16S–23S rRNA ITS region) to support consideration based on the 16S rRNA sequences analyses in determining separated species (JOHANSEN et al., 2011; MAREŠ 2018; WILLIS & WOODHOUSE 2020). The secondary structure of the 16S–23S rRNA ITS region (D1–D1′, V2, Box–B, and V3 helices) as alternate genetic autapomorphies has been largely used as an

effective characteristic to evaluate cyanobacterial taxa at the species level (Johansen et al. 2011; Hašler et al. 2014; Cai et al. 2018). This study showed that the secondary structures (D1–D1′, Box–B, and V3 helices) of the 16S–23S rRNA ITS region in operon types 1 and 2 obtained from *S. foetidum* were markedly different from the other taxa of *Scytonema* sensu stricto clade and closely related genera for which the 16S–23S rRNA ITS region data are available. Moreover, additional evidence for recognition of *S. foetidum* appeared in the high dissimilarity of the ITS region sequence. According to the descriptions of previous research, strains/sequences within the same species will have dissimilarities in the ITS region in all pairwise comparisons of less than ~ 3.0%, whereas separated species will have a dissimilarity of > 7.0 % (Erwin & Thacker 2008; Osorio–Santos et al., 2014; Mai et al. 2018; Pietrasiak et al. 2021; Berthold et al. 2021). Based on these criteria, *S. foetidum* differs uniquely from all the other *Scytonema* taxa compared, with a genetic dissimilarity of the ITS region >17.0% (< 83.0% similarity values) which is considered strong evidence for lineage separation (Table 3). Thus, all molecular data obtained in this study (e.g. phylogeny inference, 16S–23S rRNA ITS secondary structures and the genetic distance analyses) adequately support the separation of *S. foetidum* from other *Scytonema* species.

Based on the 16S rRNA phylogenetic analyses, an uncultured bacteria clone TG–32 (JQ769542, subclade S8) was the nearest lineage to the *S. foetidum* clade (subclade S9), with high 16S rRNA sequence similarity (98.4%). Since the sequence of TG–32 comes from environmental sampling of soil crust from copper mine tailings wastelands in China, we could not compare its morphology with our strains. Subclades within the *Scytonema* sensu stricto indicated that subclade S1–S3 showed a relatively large genetic distance (93.4–93.7% similarity) in the 16S rRNA sequences with the type species *S. hofmanii* (subclade S6) below the genus cutoff (<94.5% similarity) (Stackebrandt & Ebers 2006; Yarza et al. 2014; Kim et al. 2014). Noticeably, the position of *S.* cf. *mirabile* ER0515.01 (subclade S1) in the 16S rRNA and nifH trees was inconsistent, showing that *S.* cf. *mirabile* ER0515.01 is distant from the type species of *Scytonema, S. hofmanii* (subclade S6). Furthermore, many subclades (i.e. S5, S8, and S10–S11) should be designed as new *Scytonema* species, relating to the low similarity value sufficient for species cutoff (<98.7% similarity) and forming a monophyletic clade (Kim et al. 2014, Johansen et al. 2017). Unfortunately, these strains were lost, or were not cultured before investigation of the morphological features and any taxonomic traits. Therefore, adding more novel genera or species from the *Scytonema* sensu stricto clade is indispensable for future study. We hope that our genetic analyses already will help to facilitate an improved Scytonemaceae taxonomy after conducting the polyphasic investigations.

Olfactory method and geoA gene screening suggested that *S. foetidum* produced geosmin an odoriferous compound of concern which causes water to smell and taste earthy/musty. Previous studies reported that periphytic *Scytonema* sp. CHAB3651 from China could produce geosmin (Wang et al. 2019). However, the 16S rRNA phylogenetic trees undertaken in this study indicated that the Chinese strain was grouped in the *Brasilonema* clade (data not shown). In agreement with the previous studies of Wang et al. (2019), Tawong et al. (2019), and Churro et al. (2020), the geoA gene phylogenetic trees obtained in the present study showed that some cyanobacteria sequences were a co–evolved mixture which could not separate heterocyte or nonheterocyte groups. In agreement with Wang et al. (2019), this implies that horizontal gene transfer of the geoA gene may have occurred in cyanobacteria, affecting the identification and quantification of geosmin producers during environmental monitoring through detection of geo sequences. Thus, further studies on the diversity and evolution of the cyanobacterial geosmin gene and additional monitoring methods are necessary.

Results of morphological and genetic analyses suggest that *S. foetidum* differed from the type species *S. hofmanii* and all members of the *Scytonema* sensu stricto. Furthermore, *S. foetidum* produced the odoriferous compound geosmin. Consequently, we purpose *S. foetidum* nov. sp. as a novel species within the genus *Scytonema*.

Conclusion

This study performed a polyphasic taxonomic determination on two *Scytonema*–like strains (NUACC05 and NUACC06) that were isolated from a wet soil sample from the Khek River in the lower northern part of Thailand. Morphological differences, phylogenetic analyses based on the 16S rRNA, rbcLX, and nifH gene sequences as well as the unique patterns of ITS secondary structures led us to determine that our strains were differentiated from the type species *Scytonema* and other known *Scytonema* species. Evolutionary distances based on 16S rRNA sequence and 16S–23S rRNA ITS region sequences also support the novel strain as a separate *Scytonema* species. Furthermore, our strains produce the odoriferous compound geosmin. Considering all the results obtained in this study, we propose the description of *S. foetidum* sp. nov., as a novel *Scytonema* species.

References

Bornet, É. & Flahault, C. (1888): Revision des Nostocacées hétérocystées contenues dans les principaux herbiers de France (quatrième et dernier fragment). Annales des Sciences Naturelles. – Botanique,Septième Série 7: 177–262.

Berthold, D.E.; Lefler, F.W.; Huang, I–S.; Abdulla, H.; Zimba, P.V. & Laughinghouse IV, H.D. (2021): *Iningainema tapete* sp. nov. (Scytonemataceae, Cyanobacteria) from greenhouses in central Florida (USA) produces two types of nodularin with biosynthetic potential for microcystin–LR and anabaenopeptin production. – Harmful Algae 101: 101969.

Cai, F.F.; Yang, Y.; Wen, Q. & Li, R. (2018): *Desmonostoc danxiaense* sp. nov. (Nostocales, Cyanobacteria) from Danxia mountain in China based on polyphasic approach. – Phytotaxa 367: 233–244.

Casamatta, D.A. & Vis, M.L. (2004): Current velocity and nutrient level effects on the morphology of *Phormidium retzii* (Cyanobacteria) in artificial stream mesocosms. – Algological Studies 113:87–99.

Catherine, Q.; Susanna, W.; Isidora, E–S.; Mark, H.; Aurélie, V. & Jean–François, H. (2013): A review of current knowledge on toxic benthic freshwater cyanobacteria – Ecology, toxin production and risk management. – Water Research 47: 5464–5479.

Choi, H.J.; Joo, J–H.; Kim, J–H.; Wang, P.; Ki, J–S. & Han, M–S. (2018): Morphological characterization and molecular phylogenetic analysis of *Dolichospermum hangangense* (Nostocales, Cyanobacteria) sp. nov. from Han River, Korea. – Algae 33: 143–156.

Churro, C.; Semedo–Aguiar, A.P.; Silva, A.D.; Pereira–Leal, J.B. & Leite, R.B. (2020): A novel cyanobacterial geosmin producer, revising *GeoA* distribution and dispersion patterns in Bacteria. – Scientific Reports 10: 8679.

Correns, C. (1889): Ueber Dickenwachsthum durch Intussusception bei einigen Algenmembranen. – Flora (Jena) 72: 298–347.

Edgar, R.C. (2004): MUSCLE: multiple sequences alignment with high accuracy and high throughput. – Nucleic Acids Research 32: 1792–1797.

Erwin, P. & Thacker, R.W. (2008): Cryptic diversity of the symbiotic cyanobacterium *Synechococcus spongiarum* among sponge hosts. – Molecular Ecology 17: 2937–2947.

Fiore, M.F.; Sant'Anna, C.L.; Azevedo, M.T.P.; Komárek, J.; Kaštovský, J.; Sulek, J. & Lorenzi, A.S. (2007): The cyanobacterial genus *Brasilonema* molecular and phenotype evaluation. – Journal of Phycology 43: 789–798.

Godo, T.; Saki, Y.; Nojiri, Y.; Tsujitani, M.; Sugahara, S.; Hayashi, S.; Kamiya, H.; Ohtani, S. & Seike, Y. (2017): Geosmin–producing Species of *Coelosphaerium* (Synechococcales, Cyanobacteria) in Lake Shinji. Japan. Scientific Reports 7: 41928.

Guindon, S.; Dufayard, J.F.; Lefort, V.; Anisimova, M.; Hordijk, W. & Gascuel, O. (2010): New algorithms and methods to estimate maximum–likelihood phylogenies: assessing the performance of PhyML 3.0. – Systematic Biology 59: 307–321.

Hašler, P.; Dvořák, P.; Poulíčková, A. & Casamatta, D.A. (2014): A novel genus *Ammassolinea* gen.nov. (Cyanobacteria) isolate from subtropical epipelic habitats. – Fottea 14: 241–248.

Hayashi, S.; Ohtani, S.; Godo, T.; Nojiri, Y.; Saki, Y.; Esumi, T. & Kamiya, H. (2019): Identification of geosmin biosynthetic gene in geosmin–producing colonial cyanobacteria *Coelosphaerium* sp. and isolation of geosmin non–producing *Coelosphaerium* sp. from brackish Lake Shinji in Japan. – Harmful Algae 84: 19–26.

Hentschke, G.S. & Komárek, J. (2014): *Scytonema santannae*, a new morphospecies of cyanobacteria from the Atlantic rainforest, southeastern Brazil. – Brazilian Journal of Botany 37: 293–298.

Johansen, J.R. & Casamatta, D.A. (2005): Recognizing cyanobacterial diversity through adoption of a new species paradigm. – Algological Studies (Cyanobacterial Research 6) 117: 71–93.

Johansen, J.R.; Kovacik, L.; Casamatta, D.A.; Iková, K.F. & Kaštovský, J. (2011): Utility of 16S–23S ITS sequence and secondary structure for recognition of intrageneric and intergeneric limits within cyanobacterial taxa: *Leptolyngbya corticola* sp. nov. (Pseudanabaenaceae, Cyanobacteria). – Nova Hedwigia 92: 283–302.

Johansen, J.R.; Mareš, J.; Pietrasiak, N.; Bohunická, M.; Zima Jr., J.; Štenclová, L. & Hauer, T. (2017): Highly divergent 16S rRNA sequences in ribosomal operons of *Scytonema hyalinum* (Cyanobacteria). – PLoS One 12: e0186393.

Kim, K.; Park, C.; Yoon, Y. & Hwang, S.J. (2018): Harmful cyanobacterial material production in the North Han River (South Korea): Genetic potential and temperature dependent properties. – International Journal of Environmental Research and Public Health 15: 444.

Kim, M.; Oh, H.S.; Park, S.C. & Chun, J. (2014): Towards a taxonomic coherence between average nucleotide identity and 16S rRNA gene sequence similarity for species demarcation of prokaryotes. – International Journal of Systematic and Evolutionary Microbiology 64: 346–351.

Kiseleva, E. (1930): About a new bluegreen algae *Scytonematopsis woronichinii*. – Zhurnal Russkago Botanicheskago Obshchestva pri Akademii Nauk. 15: 169–174.

Komárek, J. (2013): Cyanoprokaryota. 3. Teil / 3rd part: Heterocytous Genera. – In: Ettl, H., Gerloff J., Heynig, H. & Pascher, A. (eds): Süßwasserflravon Mitteleuropa, Bd. 19/3. – 1130 pp., Springer, Berlin.

Komárek, J. & Johansen, J. (2015): Filamentous cyanobacteria. – In: Wehr, J.D., Sheath, R.G. & Kociolek, J.P. (eds): Freshwater algae of North America. Ecology and classification. – pp. 135–235, Academic Press, San Diego.

Komárek, J.; Sant'Anna, C.L.; Bohunická, M.; Mareš, J.; Hentschke, G.S.; Rigonato, J. & Fiore, M.F. (2013): Phenotype diversity and phylogeny of selected *Scytonema*–species (Cyanoprokaryota) from SE Brazil. – Fottea 13:173–200.

Komárek, J.; Kaštovský, J.; Mareš, J. & Johansen, J.R. (2014): Taxonomic classification of cyanoprokaryotes (cyanobacterial genera) 2014, using a polyphasic approach. – Preslia 86: 295–335.

Komárková, J.; Zapomělová, E. & Komárek, J. (2013): *Chakia* (cyanobacteria), a new heterocytous genus from Belizean marshes identified on the basis of the 16S rRNA gene. – Fottea 13: 227–233.

Kumar, S.; Stecher, G.; Li, M.; Knyaz, C. & Tamura, K. (2018): MEGA X: molecular evolutionary genetics analysis across computing platforms. – Molecular Biology and Evolution 35: 1547–1549.

Lowe, T.M. & Eddy, S.R. (1997): tRNAscan–SE: a program for improved detection of transfer RNA genes in genomic

sequence. – Nucleic Acids Research 25: 955–964.

MAI, T.; JOHANSEN, J.R.; PIETRASIAK, N.; BOHUNICKÁ, M. & MARTIN, P.M. (2018): Revision of the Synechococcales (Cyanobacteria) through recognition of four families including Oculatellaceae fam. nov. and Trichocoleaceae fam. nov. and six new genera containing 14 species. – Phytotaxa 365: 001–059.

MAREŠ, J. (2018): Multilocus and SSU rRNA gene phylogenetic analyses of available cyanobacterial genomes, and their relation to the current taxonomic system. – Hydrobiologia 811: 19–34.

MATHEWS LAB, University of Rochester Medical Center. (2018): RNA structure, version 6.0.1 – Available from: https://rna.urmc.rochester.edu/RNAstructure.html (accessed 16 April 2018)

MCGREGOR, G.B. (2018): Freshwater cyanobacteria of north–eastern Australia: 3. Nostocales. – Phytotaxa 359: 1–166.

MCGREGOR, G.B. & SENDALL, B.C. (2017a): *Iningainerma pulvinus* gen nov., sp nov. (Cyanobacteria, Scytonemataceae) a new nodularin producer from Edgbaston Reserve, north–eastern Australia. – Harmful Algae 62: 10–19.

MCGREGOR, G.B. & SENDALL, B.C. (2017b): *Ewamiania thermalis* gen. et sp. nov. (Cyanobacteria, Scytonemataceae), a new cyanobacterium from Talaroo thermal springs, north–eastern Australia. – Australian Systematic Botany 30: 38–47.

MCGREGOR, G.B. & SENDALL, B.C. (2021): True branching and phenotypic plasticity in the planktonic cyanobacterium *Dolichospremum branchiatum* sp. nov. (Nostocales, Aphanizomenonaceae), from south–eastern Australia. – Phytotaxa 491: 093–114.

NYLANDER, J.A.A. (2004): MrModeltest v2. Program distributed by the author. – Evolutionary Biology Centre, Uppsala University.

OKONECHNIKOV, K.; GOLOSOVA, O.; FURSOV, M. & UGENE TEAM. (2012): Unipro UGENE: a unified bioinformatics toolkit. – Bioinfromatics 28: 1166–1167.

OLSON, J.B.; STEPPE, T.F.; LITAKER, R.W.& PAERL, H.W. (1998): N2–fixing microbial consortia associated with the ice cover of Lake Bonney, Antarctica. – Microbial Ecology 36: 231–238.

OSORIO–SANTOS, K.; PIETRASIAK, N.; BOHUNICKÁ, M.; MISCOE, L.H.; KOVÁČIK, L.; MARTIN, M.P. & JOHANSEN, J.R. (2014): Seven new species of *Oculatella* (Pseudanabaenales, Cyanobacteria): taxonomically recognizing cryptic diversification. – European Journal of Phycology 49: 450–470.

PALINSKA, K.A. & SUROSZ, W. (2014): Taxonomy of cyanobacteria: a contribution to consensus approach. – Hydrobiologia 740: 1–11.

PERKERSON, R.B. III; JOHANSEN, J.R.; KOVÁČIK, L.; BRAND, J.; KAŠTOVSKÝ, J. & CASAMATTA, D.A. (2011): A unique pseudanabaenalean (cyanobacteria) genus *Nodosilinea* gen. nov. based on morphological and molecular data. – Journal of Phycology 47: 1397–1412.

PIETRASIAK, N.; REEVE, S.; OSORIO–SANTOS, K.; LIPSON, D.A. & JOHANSEN, J.R. (2021): *Trichotorquatus* gen. nov. – A new genus of soil cyanobacteria discovered from American drylands. – Journal of Phycology: In press.

SANT'ANNA, C.L.; AZEVEDO, T.M.P.; KAŠTOVSKÝ, J. & KOMÁREK, J. (2010): Two form–genera of aerophytic heterocytous cyanobacteria from Brasilian rainy forest "Mata Atlântica". – Fottea 10:217–228.

SARAF, A.; DAWDA, H.G.; SURADKAR, A.; BATULE, P.; BEHERE, I.; KOTULKAR, M.; KUMAT, A. & SINGH, P. (2018): Insights into the phylogeny of false–branching heterocytous cyanobacteria with the description of *Scytonema pachmarhiense* sp. nov. isolated from Pachmarhi Biosphere Reserve, India. – FEMS Microbiology Letters 365: 1–9.

SINGH, P.; MINZ, R.; KUNUI, K.; SHAIKH, Z.M.; SURADKAR, A.; SHOUCHE, Y.S.; MISHRA, A.K. & SINGH, S.S. (2017): A new species of *Scytonema* isolated from Bilaspur, Chhattisgarh, India using the polyphasic approach. – Plant Systematics and Evolution volume 303: 249–258

SINGH, P.; MINJ, R.A.; KUNUI, K.; SHAIKH, M.Z.; SURADKAR, A.; SHOUCHE, Y.S.; MISHRA, A.K. & SINGH, S.S. (2016): A new species of *Scytonem*a isolated from Bilaspur, Chhattisgarh, India. – Journal of Systematics and Evolution 9999: 1–9

SENDALL, B.C. & MCGREGOR, G.B. (2018): Cryptic diversity within the *Scytonema* complex: Characterization of paralytic shellfish toxin producer *Herteroscytonema crispum*, and the establishment of the family Heteroscytonemataceae (Cyanobacteria/Nostocales). – Harmful Algae 80: 158–170.

STACKEBRANDT, E. & EBERS, J. (2006): Taxonomic parameters revisited: tarnished gold standards. – Microbiology Today 4: 152–155.

SUURNÄKKI, S.; GOMEZ–SAEZ, G.V.; RANTALA–YLINEN, A.; JOKELA, J., FEWER, D.P. & SIVONEN, K. (2015): Identification of geosmin and 2–methylisoborneol in cyanobacteria and molecular detection methods for the producers of these compounds. – Water Research 68: 56–66.

TANABE, Y.; KASAI, F. &WATANABE, M. M. (2007): Multilocus sequence typing (MLST) reveals high genetic diversity and clonal population structure of the toxic cyanobacterium *Microcystis aeruginosa*. – Microbiology 153: 3695–3703.

TAWONG, W. (2017): Diversity of the potential 2–Methylisoborneol–producing genotypes in Thai strains of *Planktothricoides* (Cyanobacteria). – Brazilian Archives of Biology and Technology 60: e17160567.

TAWONG, W.; PONGCHAROEN, P.; PONGPADUNG, P. & PONZA, P. (2019): *Neowollea manoromense* gen. & sp. nov. (Nostocales, Cyanobacteria), a novel geosmin producer isolated from Thailand. – Phytotaxa 424: 1–17.

RAJANIEMI, P.; HROUZEK, P.; KASTOVSKA, K.; WILLAME, R.; RANTALA, A.; HOFFMANN, L.; KOMÁREK, J. & SIVONEN, K. (2005): Phylogenetic and morphological evaluation of the genera *Anabaena*, *Aphanizomenon*, *Trichormus* and *Nostoc* (Nostocales, Cyanobacteria). – International Journal of Systematic and Evolutionary Microbiology 55: 11–26.

RONQUIST, F.; TESLENKO, M.; VAN DER MARK, P.; AYRES, D.L.; DARLING, A.; HÖHNA, S.; LARGET, B.; LIU, L.; SUCHARD, M.A. & HUELSENBECK, J.P. (2012): MrBayes 3.2: Efficient Bayesian phylogenetic inference and model choice across a large model space. – Systematic Biology 61: 539–542.

RUDI, K.; SKULBERG, M.O. & JAKOBSEN K.S. (1998): Evolution of cyanobacteria by exchange of genetic material among phylogenetically related strains. – Journal of Bacteriology 180: 3453–3461.

WANG, Z.; SONG, G.; LI, Y.; YU, G.; HOU, X.; GAN, Z. & LI, R. (2019): The diversity, origin, and evolutionary analysis of geosmin synthase in cyanobacteria. – Science of the Total Environment 689: 789–796.

WILLAME, R.; BOUTTE, C.; GRUBISIC, S.; WILMOTTE, A.; KOMÁREK, J. & HOFFMANN, L. (2006): Morphological

and molecular characterization of planktonic cyano-
bacteria from Belgium and Luxembourg. – Journal of
Phycology 42: 1312–1332.

Willis, A. & Woodhouse, J.N. (2020): Defining cyanobacterial
species: diversity and description through genomics.
– Critical Reviews in Plant Sciences 39: 101–124.

Whitton, B.A. (2012): Ecology of Cyanobacteria II: Their
Diversity in Space and Time. – 760 pp., Springer, London.

Wu, X.; Jiana, J.; Wan, Y.; Giesy, J.P. & Hua, J. (2012):
Cyanobacteria blooms produce teratogenic retinoic acids.
– Proceedings of the National Academy of Sciences of
the United States of America 109: 9477–9482.

Yamamoto, Y. (2011): Elucidating the adhesion and growth of
the green alga *Scenedsmus acutus* under culture condi-
tion by using ultrasonic treatment. –Taiwania 56: 1–6.

Yarza, P.; Yilmaz, P.; Pruesse, E.; Glöckner, F.O.; Ludwig,
W.; Schleifer, K.; Whitman, W.B.; Euzéby, J.;
Amann, R. & Rosselló–Móra, R. (2014): Uniting
the classification of cultured and uncultured bacteria
and archaea using 16S rRNA gene sequences. – Nature
Reviews Microbiology 12: 635–645.

Żyszka–Haberecht, B.; Niemczyk, E. & Lipok, J. (2019):
Metabolic relation of cyanobacteria to aromatic com-
pounds. – Applied Microbiology and Biotechnology
103: 1167–1178.

Supplementary material

The following supplementary material is available for this article:

Supplementary information, Table S1, S2, Figs S1, S2.

This material is available as part of the online article (http://
fottea.czechphycology.cz/contents)